# Supplementary Materials

## Supplementary Note 1

### Mechanism of the phase-sensitive detection of stimulated Raman scattering signal

Here we explain the mechanism of the phase sensitive detection of stimulated Raman scattering signal. In essence, SRS signal is a loss of the pump (excitation) beam (called stimulated Raman loss (SRL)) and thus, demands a prior requirement to extract this "loss" from the excitation signal. The detection strategy is to modulate the intensity of the Stokes beam so that there will be a periodic overlap between the pump and Stokes beams (Figure. S1). Since the SRS process occurs only when the two beams overlap together, the pump beam will experience a periodic SRL with the modulated Stoke beam. Therefore, the lock-in amplifier can demodulate SRL from the pump beam for phase-sensitive detection. For the implementation of the phase-sensitive detection, we employ electro-optical modulator (EOM) to modulate the Stokes beam and a lock-in amplifier to demodulate SRL from the pump beam based on the reference frequency from the EOM, as described in Figure 1. We choose 20 MHz as modulation frequency to minimize interferences (e.g., 1/f noise, laser power fluctuations, etc) of fs laser sources [1].

## Supplementary Note 2

### The principle of a spectral focusing technique for hyperspectral SRS imaging

Here we explain the rationale for the use of the spectral focusing technique in Figure 1. The laser source used in Figure 1 gives 100 fs laser with the spectral width of (~150 $cm^{-1}$) being broader than the average Raman bandwidth (~15 $cm^{-1}$). As a result, the laser source itself offers a poor spectral resolution, leading to a low chemical specificity. To resolve the issue, we employ the spectral focusing technique by adding glass rods into the SRS system [2]. The objective is to: i) improve spectral resolution, and ii) facilitate hyperspectral scanning by changing the temporal differences between the pump and Stokes beams. The glass rods are placed in the excitation beam paths so that when the beams pass through them, they will

experience a significant degree of group velocity dispersion with their pulsewidth 'chirping' (broadening) according to

$$\tau = \tau_o \sqrt{1 + \left(\frac{4 \ln|k|z}{\tau_o}\right)^2}$$

where $\tau_o$ is the initial pulse width and z is the length of the glass rod. k is the group velocity parameter defined as

$$\mathrm{k} = \frac{\lambda^3}{2\pi c^2} \frac{d^2 n}{d\lambda^2}$$

where n is refractive index. Subsequently, the spectral resolution ($\boldsymbol{\sigma_D}$) is improved based on the following equation

$$\sigma_D = 4\sqrt{\ln 2}\,/\tau$$

Given the SF-57 glass rods with the lengths of 48 and 50 cm for pump and Stokes beam paths, respectively, the resultant pulse widths of the pump and Stokes beams would be 1.7 and 2 ps, respectively, in our SRS system. These correspond to the spectral resolution of ~ 15 $cm^{-1}$ for SRS signal, which is sufficient for efficient resonance with the Raman peaks in the high wavenumber range.

Further, given the instantaneous frequency difference,

$$\omega_D(t) = \omega_{pump} - \omega_{stokes} + 2\beta t_0$$

where $t_0$ is an inter-pulse delay between the pump and Stokes beams, and β is the linear chirp parameter as defined in the following:

$$\beta(\mathrm{z}) = \frac{8(ln2)^2|k|z}{\tau_o^2 \tau^2}$$

Therefore, the Raman shift can be tuned by changing $t_0$. We add in a time delay line in the pump beam path, which can be automatically controlled with a minimum step size of 20 μm; and it corresponds to a step size of 7.5 $cm^{-1}$ that has a sufficiently small Raman scanning interval for hyperspectral SRS imaging.

**Supplementary Note 3**

**Measurement of bacterial growth**

Bacterial growth curves at the exponential growth phase are measured and compared under the conditions of absence of vancomycin and presence of pure vancomycin to assess the retention of the inhibitory effect of vancomycin after conjugation with aryl-alkyne Raman tag (n=3). Three reagents (pure vancomycin, van-PEPEA and PBS) are added to separate samples from the same culture, and the optical density@600 nm of each sub-sample is measured at the indicated time points of 0, 30, 60 and 120 min, respectively. The incubation concentrations of vancomycin and van-PEPEA are set at the minimum inhibitory concentration (10 μg/ml).

**Supplementary Note 4**

**Chemicals and alkyne Raman tag synthesis**

Boc-tyramine, Trifluoromethanesulfonic anhydride (TFO), $Pd(PPh_3)_2Cl_2$, CuI, trimethylamine (TEA), ethynylbenzene, 1-Hydroxybenzotriazole hydrate (HOBT), Vancomycin (Van), and 4M HCl in dioxane were purchased from Sigma-Aldrich. All other chemicals were reagent grade and used as received. Nuclear magnetic resonance (NMR) spectra were recorded on Varian 600.

**1. Synthesis of 2-(4-(phenylethynyl)phenyl)ethan-1-amine (PEPEA)**

PEPEA was synthesized according to Scheme 1; three steps were involved in the synthesis as follows:

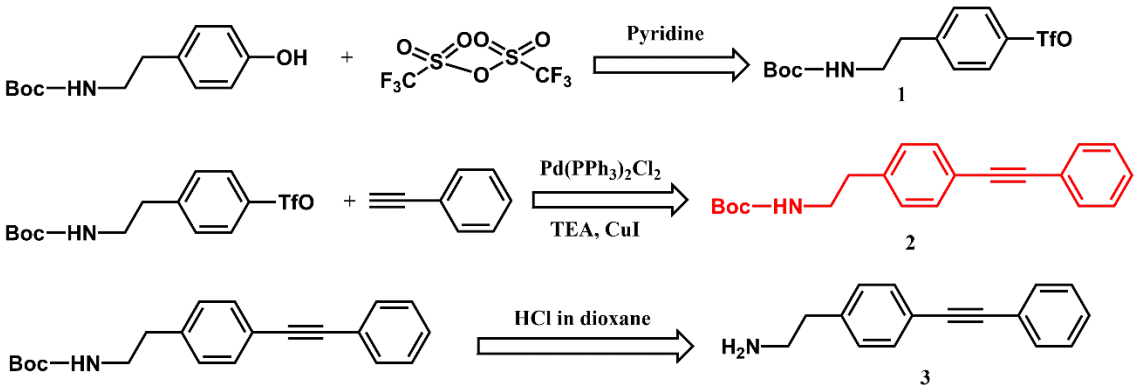


**Scheme 1.** Synthesis of PEPEA.

**Step 1.1. 4-(2-((tert-butoxycarbonyl)amino)ethyl)phenyl trifluoromethanesulfonate (BAEPT,chemical 1)**

N-Boc-tyramine (15 g, 63.2 mmol) was dissolved in 100 ml dichloromethane containing pyridine (24 ml, 316 mmol), followed by stirring the mixture in ice water for 10 min. Trifluoromethanesulfonic anhydride (17.2 mL, 94.8 mmol) in 50 mL DCM was added dropwise in 1 hr. The final mixture was stirred in ice water for 2 hr and room temperature for another 6 hr. The mixture was subsequently washed with 0.1 M $CuSO_4$ aqueous solution, 0.1 M NaOH and saline three times. The collected organic phase was dried over anhydrous $Na_2SO_4$. The organic solvent was removed by rotary evaporator, and the crude product was purified by column chromatography (Hexane/AcOEt=10/1) to give BAEPT as a white crystal. Yield: 95%. $^1$H NMR (600 MHz, $CDCl_3$): 7.6 (2H, m), 7.2 (2H, d), 3.37 (2H, t), 2.82 (2H, t), 1.43 (9H, s).

**Step 1.2. Tert-butyl (4-(phenylethynyl)phenethyl)carbamate (TPEPC, Chemical 2)**

BAEPT (11.4 g, 31 mmol), ethynylbenzene (9.4 g, 92 mmol) and triethylamine (TEA) (50 mL) were dissolved in a flask containing 250 mL DMF. After bubbling $N_2$ for 10 min,

$Pd(PPh_3)_2Cl_2$ (2.3 g, 3.1 mmol) and CuI (600 mg, 3.1 mmol) were added. The mixture was stirred at 110 ºC for 8 hr. The reaction mixture was filtered through a pad of Celite, and the combined filtrate was concentrated under reduced pressure. The crude mixture was purified by column chromatography (Hexane/AcOEt= 20 /1) to give TPEPC (81%) as a pale yellow powder. $^1$H NMR (600 MHz, $CDCl_3$): 7.52-7.48 (4H, m), 7.39 (3H, d), 7.31(2H, d), 3.36 (2H, t), 2.82 (2H, t), 1.42 (9H, s).

**Step 1.3. 2-(4-(phenylethynyl)phenyl)ethan-1-amine (PEPEA, chemical 3)**

5g TPEPC was dissolved in 5 mL DCM, the solution was added dropwise into 50 mL 4M HCl in dioxane. After 4 hr incubation, the precipitate was collected and washed with diethyl ether 3 times. The PEPEA was collected as a white crystal after drying in vacuum overnight. Yield 96%. $^1$HNMR (600 MHz, DMSO-$d_6$): 7.52-7.48 (4H, m), 7.39 (3H, d), 7.31(2H, d), 3.00 (2H, t), 2.95 (2H, t).

**2. Synthesis of Van-PEPEA**

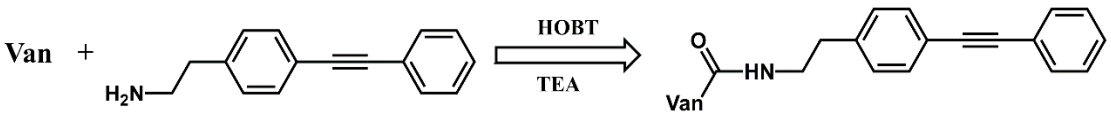


**Scheme 2.** Synthesis of Van-PEPEA.

Van-PEPEA was synthesized according to Scheme 2. Vancomycin (100 mg, 0.069 mmol ), PEPEA (g, 0.69 mmol), 1-Hydroxybenzotriazole hydrate (HOBT) (18.6 mg, 0.138 mmol) was dissolved in 5 mL DMSO, subsequently, 0.5 mL TEA (1.4 mmol) was added, the mixture was stirred at room temperature for 12 hr, the solution was washed with diethyl ether, finally precipitated into 5 mL DCM, the precipitate was collected by centrifugation. The pellet was collected after drying in vacuo overnight. Yield:97%. 1H-NMR (600 MHz,

DMSO-$d_6$): 10.28 (br s), 10.22 (s), 10.27 (s), 9.43 (br s), 9.12(br s), 8.68 (br s), 8.60 (br s), 8.18 (s), 7.97(s), 7.79 (d), 7.50-7.55 (overlapped), 7.28-7.40 (overlapped), 6.82 (s), 6.62 (s), 6.45 (s), 6.09 (br s),5.81 (br s), 5.57 (s), 5.39 (s), 5.27 (s), 5.18 (br s), 4.90 (br s), 4.70 (d, 5.7Hz ), 4.30-4.38 (overlapped), 4.03-4.14 (overlapped), 3.00 (t), 2.95 (t), 0.85-0.95 (overlapped). MS (ESI) m/z: calcd for C82H88N10O23: 1650.540 , [M+2H]/2= 826.27; [M+2H]/2 found: 826.28. The graphs of NMR and MS are available in Figure S6.

**Supplementary Note 5**

**Derivation of diffusion model for van-PEPEA penetration into the biofilm**

We propose an analytical model to describe the penetration of van-PEPEA into the biofilm for determining the diffusion constant of the biofilm. We assume that the phenomenon is governed by the two major physical processes, i.e., the diffusion and binding to the biofilm components (bacteria and EPS). The diffusion is determined based on Fick's second law,

$$\frac{\partial N_v(z,t)}{\partial \mathrm{t}} = -D\frac{\partial^2 N_v(z,t)}{\partial \mathrm{t}^2} \quad (1)$$

where $N_v$ = quantity of unbound van-PEPEA in the biofilm, and D = diffusion constant. We assume that: i) there is a constant source of van-PEPEA ($N_{media}$) on the biofilm surface, and ii) van-PEPEA cannot reach the other end of biofilm within the measurement time window (~ 60 min). In other words, the biofilm is considered as infinitely thick. Then Fick's second law can be simplified into

$$N_v(z,t) = erfc(\frac{z}{2\sqrt{Dt}}) \times N_{media}$$

To take into account the binding to the bacteria and EPS, the law of mass action can be employed. Since we assume that $N_v$ is sufficiently large, the equation becomes

$$\frac{\mathrm{d}N_{vB}}{\mathrm{dt}} = kN_v(N_{B0} - N_{vB})$$

where $N_{vB}$ = quantity of bound van-PEPEA, $N_{B0}$ = total number of binding sites of bacteria and EPS and k = rate constant.

$N_{vB}$ is proportional to the SRS intensity of van-PEPEA ($I_v$), and $N_{B0}$ is contributed by the MCR-retrieved concentration maps of S. aureus ($I_{SA}$) and EPS ($I_{EPS}$) with some respective weightages (i.e. $N_{B0} = \alpha\ I_{SA} + \beta\ I_{EPS}$). These weightages can be determined by the average colocalization coefficients obtained from Figure 4C (0.6 for S. aureus; 0.4 for EPS). Thus, the law of mass action becomes

$$C_1\frac{\mathrm{d}I_v}{\mathrm{dt}} = kN_v(C_2(0.6\mathrm{I_{SA}} + 0.4\mathrm{I_{EPS}}) - C_1I_v) \quad (2)$$

Finally, we substitute (1) into (2),

$$\frac{\mathrm{d}I_v}{\mathrm{dt}} = A_1 erfc(\frac{z}{2\sqrt{Dt}})(A_2(0.6\mathrm{I_{SA}} + 0.4\mathrm{I_{EPS}}) - I_v) \quad (3)$$

where $A_1 = \frac{kN_{media}}{C_1}$ and $A_2 = \frac{C_2}{C_1}$. Eq. 3 is solved by ODE solver for non-stiff differential equations provided by Matlab. $I_v$, $I_{SA}$ and $I_{EPS}$ are the average pixel intensities belonging to certain z and t.

**References**

1. Ozeki Y, Dake F, Kajiyama S, Fukui K, Itoh K. Analysis and experimental assessment of the sensitivity of stimulated Raman scattering microscopy. Opt Express. 2009; 17:

3651-3658.

2. Fu D, Holtom G, Freudiger C, Zhang X, Xie XS. Hyperspectral imaging with stimulated Raman scattering by chirped femtosecond lasers. J Phys Chem B. 2013; 117: 4634-4640.

**Supplementary Figures**

**Supplementary Figure S1**. Phase-sensitive detection scheme to extract stimulated Raman loss from the pump beam.

**Supplementary Figure S2**. Spontaneous Raman spectrum of van-PEPEA in the silent region (1800-2800 $cm^{-1}$ with a step size of 0.8 $cm^{-1}$) obtained by using micro-Raman spectroscopy (Invia, Renishaw).

**Supplementary Figure S3.** Average SRS spectrum of S. aureus biofilm in the high wavenumber region (2830-2980 $cm^{-1}$ with a step size of 15 $cm^{-1}$). The spectrum is acquired by averaging all the pixel intensities (128x128) across the Raman shifts scanned.

**Supplementary Figure S4**. Calibration curve for van-PEPEA. SRS intensity is plotted against van-PEPEA concentration (black) and then fitted with linear regression.

**Supplementary Figure S5.** Validation of MCR decomposition of S.aureus biofilm. Fluorescence images (A: Syoto 9 and D: Fluorescein labeled Aleuria Aurantia Lectin (AAL)) obtained using two-photon excitation fluorescence (TPEF) microscopy are spatially correlated with SRS image acquired at Raman shift of 2935cm-1

representing bacteria (B and E). (C and F) Overlay images between A and B and D and E respectively. There is a high degree of co-localization between TPEF and SRS images for bacteria, whereas the overlay between D and E suggests that EPS is covering bacterial regions in a non-uniform manner. For SRS imaging, the average powers of the pump beam (798 nm) and Stokes beam (1041 nm) on the samples are 10 and 40 mW respectively. TPEF images (A and B) are obtained by excitation at 800 nm and 970 nm (20mW) and collecting emission with 540/60 bandpass filter (Semrock) respectively. All images are obtained within 15 s with 9.6 µs of pixel dwell time for 128 x 128 pixels (40 x 40 µm) and averaging 4 times. Scale bar = 5 µm.

**Supplementary Figure S6.** Graphs of (A) NMR and (B) mass spectroscopy for characterization of van-PEPEA.

**Supplementary Videos**

**Supplementary Movie S1.** Supplementary Movies of hyperspectral SRS images scanning from 2830- 2980 $cm^{-1}$ at 15 $cm^{-1}$ intervals for S. aureus biofilm. The entire stack is obtained within 40 s with 19.6 µs of pixel dwell time for 128 x 128 pixels (40 x 40 µm).

**Supplementary Movie S2.** Three-dimensional rotation displaying S. aureus biofilm resolved into cells (green) and EPS (blue). A hyperspectral SRS image stack is z-scanned with an interval of 1.5 µm for 21 µm (40 x 40 x 21 µm).

**Supplementary Movie S3**. x-z views (40 x 21 µm) of van-PEPEA penetration into S. aureus biofilm as a function of time (0 to 60 min with an interval of 5 min).

**Supplementary Movie S4**. Concentration map (40 x 21 µm) of van-PEPEA penetration obtained by applying the calibration curve (**Supplementary Fig. S3**) to **Supplementary Movie S2**.

**Supplementary Fig. S1**

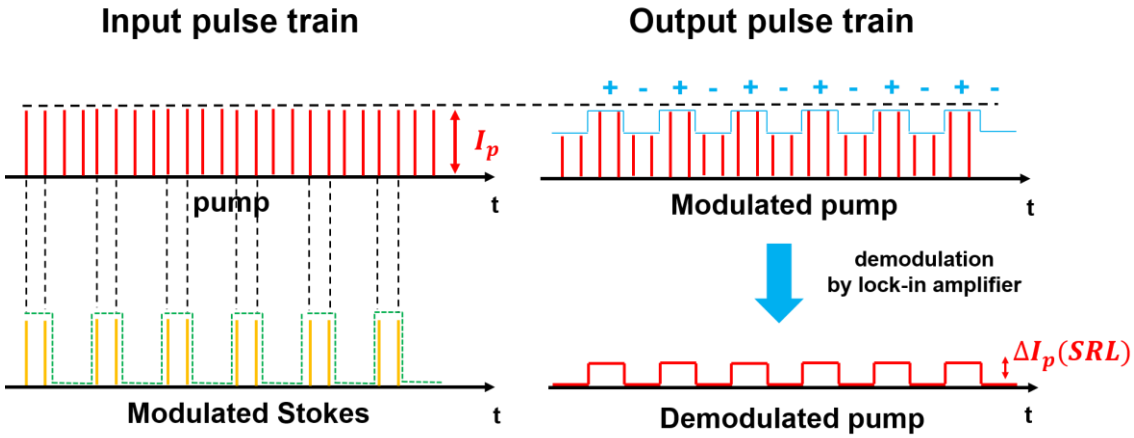

**Supplementary Fig. S2**

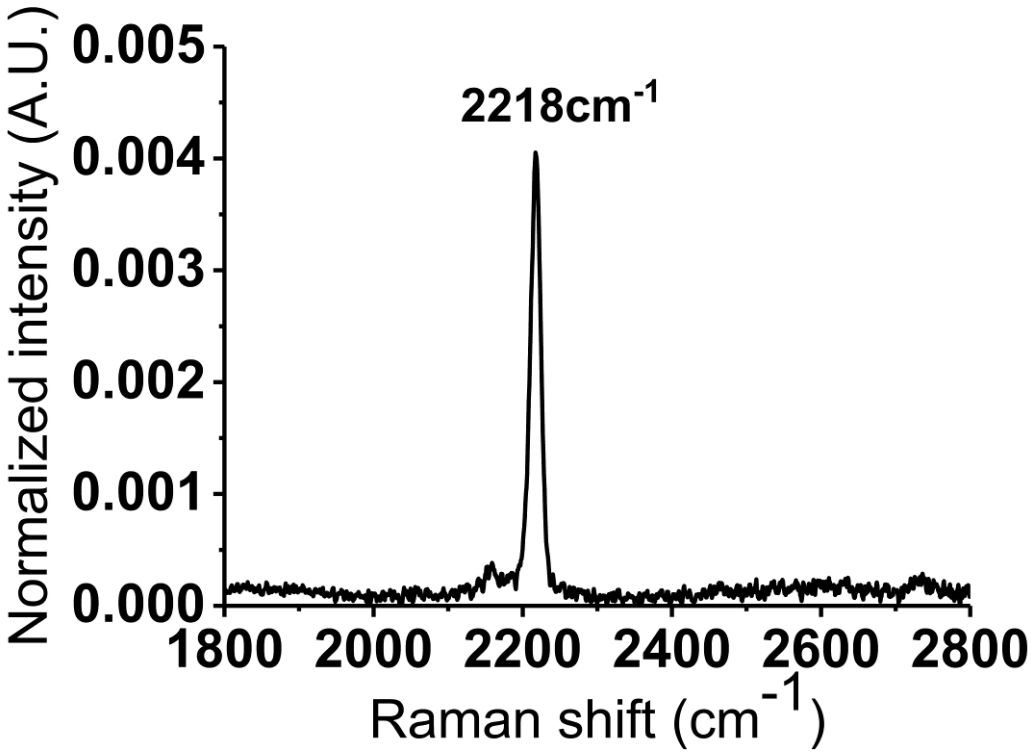

**Supplementary Fig. S3**

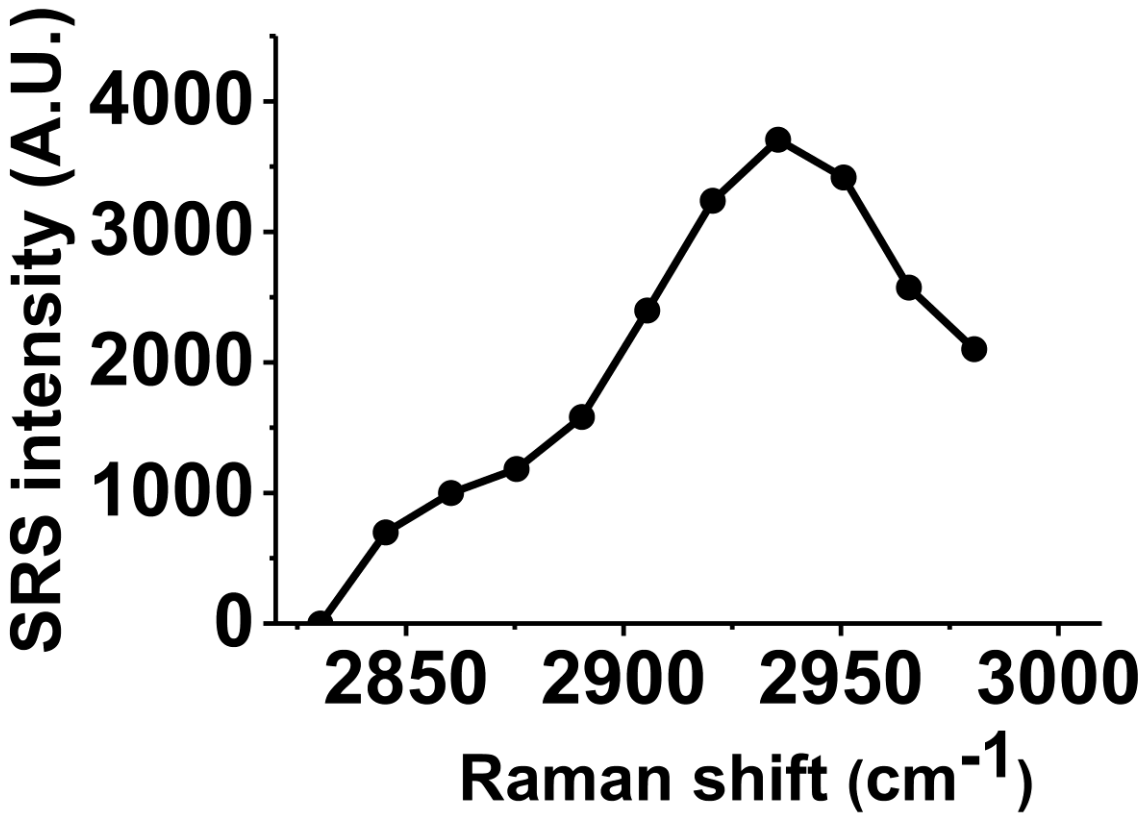

**Supplementary Fig. S4**

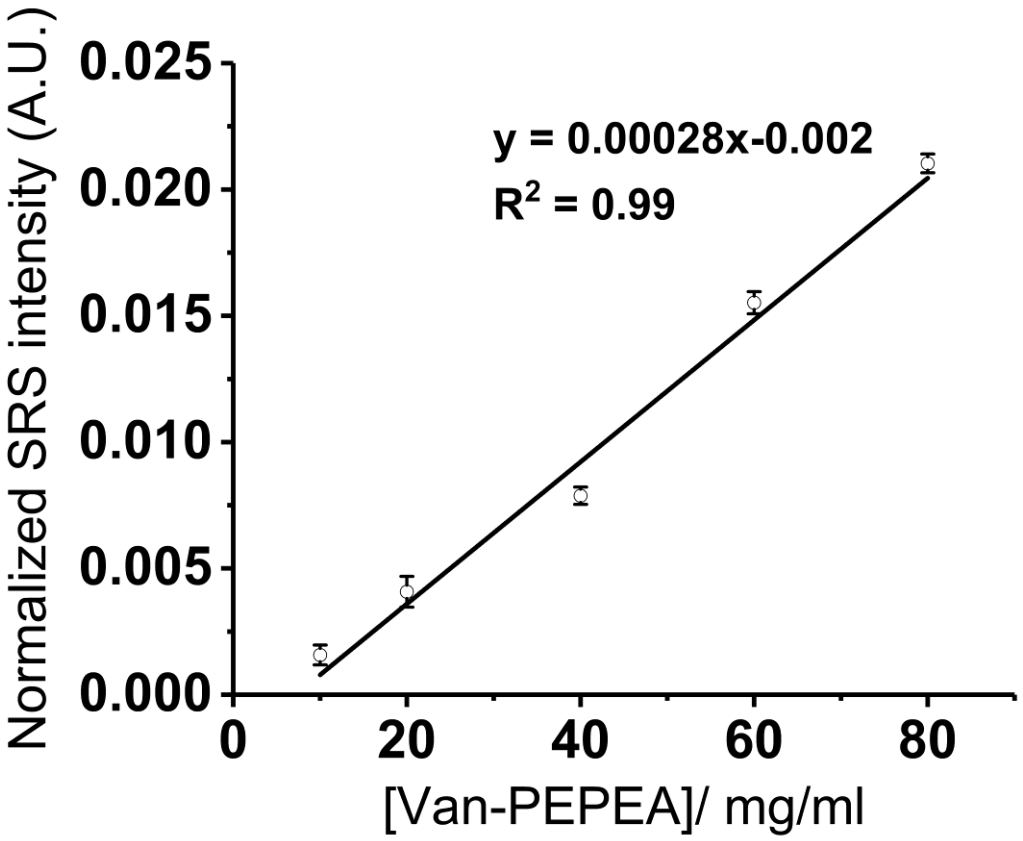

**Supplementary Fig. S5**

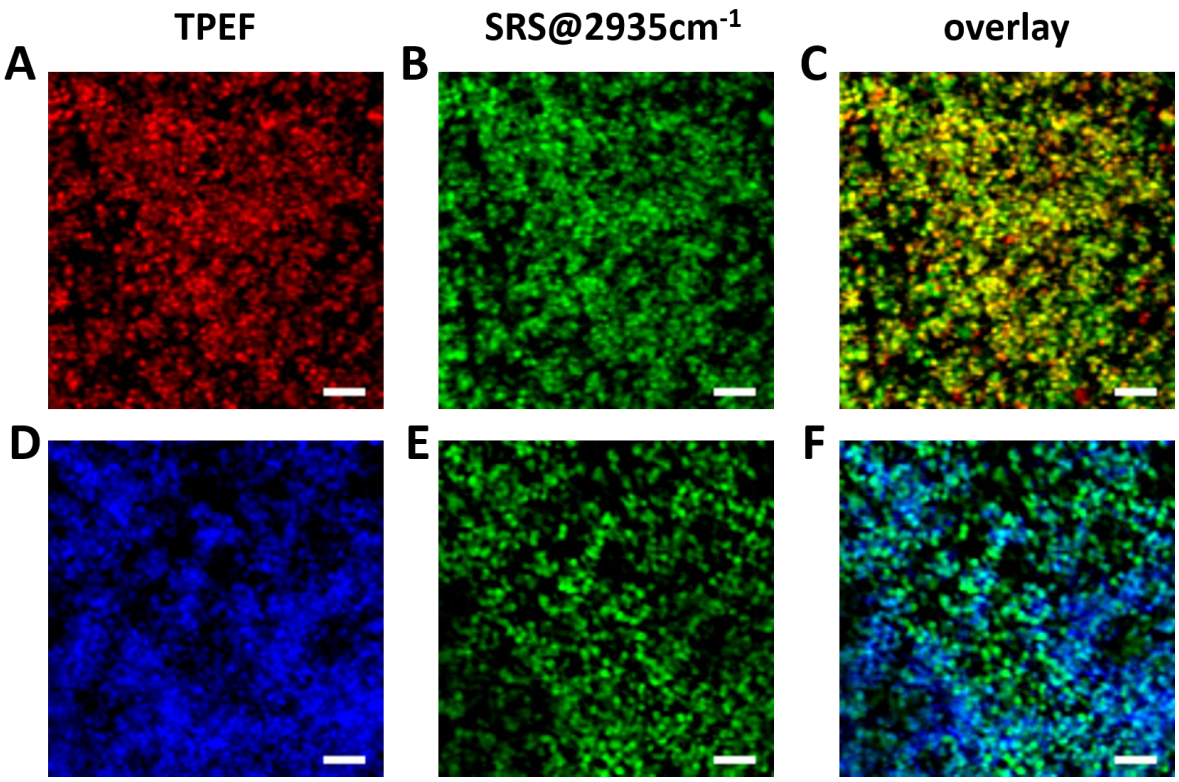
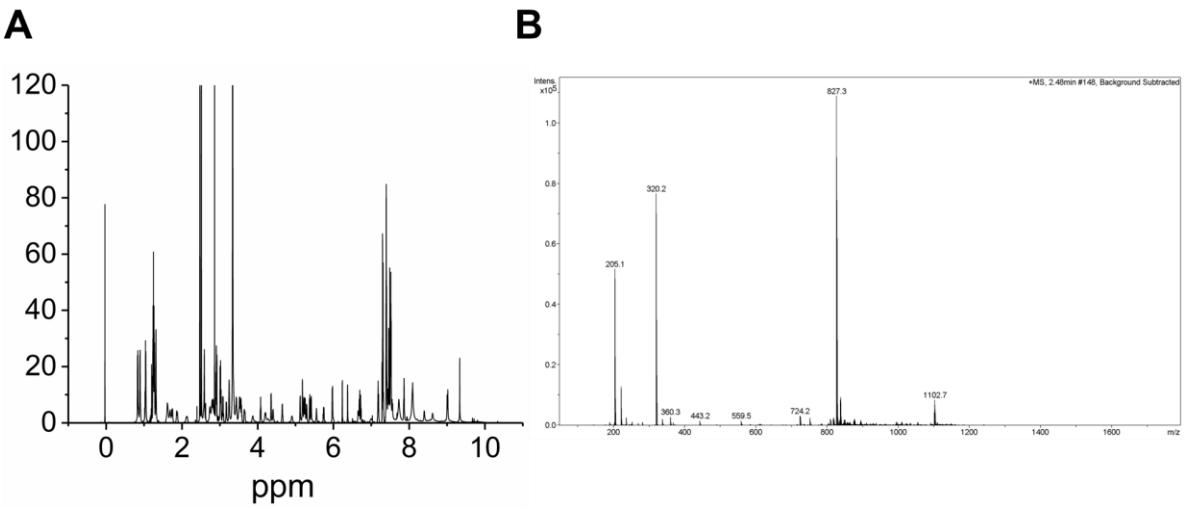
**Supplementary Fig. S6**